AFCEC-CX-TY-TR-2016-0016

PHYSIOLOGICAL AND GROWTH CHARACTERISTICS OF SHEWANELLA SPECIES

Karen Farrington, D. Matthew Eby, Susan Sizemore, Robert Nichols, & Heather Luckarift
Universal Technology Corporation
1270 N. Fairfield Road
Dayton, Ohio 45432

De'Lisa Maybin, Lloyd Nadeau, & Glenn Johnson
Air Force Research Laboratory
139 Barnes Dr, Suite 2
Tyndall AFB, Florida 32403

Guinevere Strack
Oak Ridge Institute for Science & Education
1299 Bethel Valley Road
Oak Ridge, Tennessee 37830

Contract No. FA4819-11-C-0003

May 2016

AIR FORCE CIVIL ENGINEER CENTER
READINESS DIRECTORATE

■ **Requirements & Acquisition Division** ■ **United States Air Force** ■ **Tyndall Air Force Base, FL 32403-5323**

DISCLAIMER

Reference herein to any specific commercial product, process, or service by trade name, trademark, manufacturer, or otherwise does not constitute or imply its endorsement, recommendation, or approval by the United States Air Force. The views and opinions of authors expressed herein do not necessarily state or reflect those of the United States Air Force.

This report was prepared as an account of work sponsored by the United States Air Force. Neither the United States Air Force, nor any of its employees, makes any warranty, expressed or implied, or assumes any legal liability or responsibility for the accuracy, completeness, or usefulness of any information, apparatus, product, or process disclosed, or represents that its use would not infringe privately owned rights.

NOTICE AND SIGNATURE PAGE

Using Government drawings, specifications, or other data included in this document for any purpose other than Government procurement does not in any way obligate the U.S. Government. The fact that the Government formulated or supplied the drawings, specifications, or other data does not license the holder or any other person or corporation; or convey any rights or permission to manufacture, use, or sell any patented invention that may relate to them.

This report was cleared for public release by the AFCEC Public Affairs Office at Joint Base San Antonio-Lackland Air Force Base, Texas available to the general public, including foreign nationals. Copies may be obtained from the Defense Technical Information Center (DTIC) (http://www.dtic.mil).

AFCEC-CX-TY-TR-2016-0034 HAS BEEN REVIEWED AND IS APPROVED FOR PUBLICATION IN ACCORDANCE WITH ASSIGNED DISTRIBUTION STATEMENT.

//SIGNED//	//SIGNED//
Michael Henley	Joseph Wander
Contracting Officer Representative	Technical Advisor

This report is published in the interest of scientific and technical information exchange, and its publication does not constitute the Government's approval or disapproval of its ideas or findings.

REPORT DOCUMENTATION PAGE

Form Approved
OMB No. 0704-0188

PLEASE DO NOT RETURN YOUR FORM TO THE ABOVE ADDRESS.

1. REPORT DATE *(DD-MM-YYYY)*	2. REPORT TYPE	3. DATES COVERED *(From - To)*
11-05-2016	Technical Report	01 March 2012 - 01 March 2014

4. TITLE AND SUBTITLE

Physiological and growth characteristics of Shewanella species

5a. CONTRACT NUMBER

FA4819-11-C-0003

5b. GRANT NUMBER

5c. PROGRAM ELEMENT NUMBER

6. AUTHOR(S)

Karen Farrington (1), De'Lisa Maybin (3), D. Matthew Eby (1), Susan Sizemore (1), Guinevere Strack (2), Lloyd Nadeau (3), Robert Nichols (1), Glenn Johnson (3), Heather Luckarift (1)

5d. PROJECT NUMBER

5e. TASK NUMBER

5f. WORK UNIT NUMBER

7. PERFORMING ORGANIZATION NAME(S) AND ADDRESS(ES)

(1) Universal Technology Corporation, 1270 N. Fairfield Road, Dayton, OH 45432
(2) Oak Ridge Institute for Science & Education, 1299 Bethel Valley Rd, Oak Ridge, TN 37830
(3) Air Force Research Laboratory, 139 Barnes Dr. Suite 2, Tyndall AFB, FL 32403

8. PERFORMING ORGANIZATION REPORT NUMBER

9. SPONSORING/MONITORING AGENCY NAME(S) AND ADDRESS(ES)

Air Force Civil Engineer Center
Readiness Directorate
Requirements and Acquisition Division
139 Barnes Drive, Suite 1
Tyndall Air Force Base, FL 32403-5323

10. SPONSOR/MONITOR'S ACRONYM(S)

AFCEC/CXA

11. SPONSOR/MONITOR'S REPORT NUMBER(S)

AFCEC-CX-TY-TR-2016-0016

12. DISTRIBUTION/AVAILABILITY STATEMENT

A: Approved for public release; distribution unlimited.

13. SUPPLEMENTARY NOTES

Document contains color images. Ref Public Affairs Case # AFCEC-201612, 3 June 2016.

14. ABSTRACT

This report summarizes technical effort to understand microbial interactions relevant to operational use in the marine environment. Firstly, *Shewanella frigidimarina* was investigated as a potential microbial fuel cell (MFC) catalyst. *S. frigidimarina* is halotolerant and can grow at temperatures in the range of 0-28 °C. The physiological characteristics of *S. frigidimarina* as a psychrophile provide opportunity for energy generation at unconventional operating temperatures. Secondly, the unusual growth characteristics of another *Shewanella* sp., *Shewanella japonica*, were investigated. *S. japonica* is also a halotolerant and metabolically diverse species and was investigated for its ability to form complex biofilms on solid surfaces in marine environments.

15. SUBJECT TERMS

Shewanella, Microbial Fuel Cell, Psychrophile, Shewanella japonica, Shewanella frigidimarina

16. SECURITY CLASSIFICATION OF:			17. LIMITATION OF ABSTRACT	18. NUMBER OF PAGES	19a. NAME OF RESPONSIBLE PERSON
a. REPORT	b. ABSTRACT	c. THIS PAGE			Michael V. Henley
U	U	U	SAR	33	19b. TELEPHONE NUMBER *(Include area code)*

Reset

TABLE OF CONTENTS

LIST OF FIGURES

Page

1. SUMMARY

This report summarizes technical effort performed by Universal Technology Corporation (UTC) under prime contract FA4819-11-C-0003 supported by and conducted at the Air Force Research Laboratory, Tyndall AFB, FL. Particular emphasis throughout is the integration and interaction of halotolerant microbial species with solid materials. The aim was to understand microbial interactions relevant to operational use in the marine environment. This report summarizes research and development in two primary areas (which are reported as two distinct sections). Firstly, *Shewanella frigidimarina* was investigated as a potential microbial fuel cell (MFC) catalyst (Section 2.0). *S. frigidimarina* is halotolerant and can grow at temperatures in the range of 0–28 °C. The physiological characteristics of *S. frigidimarina* as a psychrophile provide opportunity for energy generation at unconventional operating temperatures.

Secondly, the unusual growth characteristics of another *Shewanella* sp., *S. japonica*, were investigated (Section 3.0). *S. japonica* is also a halotolerant and metabolically diverse species and was investigated for its ability to form complex biofilms on solid surfaces in marine environments. Scanning electron micrographs of aluminum coupons revealed that the cells grew in a unique twisted morphology in the presence of agarose. The spiral morphology appeared sporadically, with individual cells switching between straight rods to spirals during cell elongation. The cell features are not consistent with any known physiological function of *Shewanella* but may be linked to specific nutrients in the growth medium.

The work describes how understanding fundamental biological and biophysical phenomena can be used to develop rational biotechnology solutions for Air Force requirements.

2. Physiological Characteristics of *Shewanella frigidimarina* as a Microbial Fuel Cell Catalyst

2.1. Introduction

Conventional fuel cells use inorganic catalysts and precious metals in anodic and cathodic half-reactions separated by a barrier that selectively allows passage of positively charged ions. MFCs follow the same basic principle but whole microbial cells catalyze the electrochemical processes by harvesting energy from environmental sources (such as wastewater or aquatic sediments) [1–6]. MFCs require continuous maintenance of whole living cells to sustain physiological processes, and as a result dictate stringent working conditions to maintain output. In the cathode, substrates such as molecular oxygen (O_2), or hydrogen peroxide (H_2O_2), are reduced. In combination with the anodic reaction, this process generates electrical power (voltage and current). MFC power production is a fortuitous byproduct of microbial metabolism; the ability to effectively transfer electrons is intrinsically linked to microbial mechanisms that allow the bacterium to respond to changes in physiological conditions. It is unclear, however, how specific electron transfer mechanisms are controlled by physiological constraints and environmental conditions. Elucidating and understanding these relationships may lead to improved MFC systems by: 1) guiding the rational development of engineered surfaces to improve the physical association between microbes and products of metabolism; 2) determining microbial culture conditions that provide reproducible redox processes; and thereby 3) defining optimal operational conditions for MFCs.

Shewanella frigidimarina is a facultative anaerobic, dissimilatory metal-reducing bacteria, originally isolated from Antarctic sea ice [7]. *S. frigidimarina* uses two known mechanisms to transfer electrons to insoluble electron acceptors: intermolecular electron transfer via tetraheme cytochromes, and extracellular electron transfer through mediators such as riboflavin [8–11]. These mechanisms can be exploited to produce power in MFCs [12]. *S. frigidimarina* is a psychrotroph with a reported growth range extending from 0–28 °C. It has the capability to utilize a wide variety of substrates; nitrate, nitrite, fumarate and elemental sulfur, as terminal electron acceptors for anaerobic respiration. In addition, *S. frigidimarina* is halotolerant and is therefore considered as an organism suited to producing power in MFCs that can be deployed in a marine environment at a range of environmental operating temperatures [13–17].

2.2. Methods, Assumptions, and Procedures

2.2.1. Bacterial Strains and Growth Conditions

All chemicals were obtained from Sigma–Aldrich (St. Louis, MO) unless otherwise noted. Cultures of *S. frigidimarina* (ATCC strain 700753, American Type Culture Collection, Manassas, VA) were grown in either Marine Broth 2216 (MB) (Becton, Dickinson, and Co., Franklin Lakes, NJ) or modified marine broth (MMB), containing (per L): 9.76 g NaCl, 2.5 g peptone, 3.05 g $MgCl_2$, 1.56 g $MgSO_4$, 0.89 g $CaCl_2$, 0.5 g yeast extract (pH 7.3). MMB was used in experiments to exclude riboflavin from the initial culture media. [12]. Cultures were grown overnight at 25 °C with shaking (200 rpm) and growth monitored by measuring the optical density at 600 nm (Cary 3E spectrophotometer, Varian, Palo Alto, CA). At late exponential phase, cultures were harvested by centrifugation (Sorvall RC5B Plus centrifuge,

Thermo Fisher Scientific, Waltham, MA), washed and resuspended in phosphate buffered saline (PBS) containing (per L): 8 g NaCl, 0.2 g KCl, 1.44 g Na_2HPO_4, 0.24 g KH_2PO_4 (adjusted to pH 7.4) to an optical density (OD_{600}) ~5. Cell counts were determined by conventional serial dilution, plating and colony counting to determine colony-forming units per mL (CFU mL^{-1}).

S. frigidimarina was inoculated from overnight culture into *ez*-Control bioreactors (Applikon Biotechnology BV, Nieuwpoortweg 12, The Netherlands), equipped with a 2-L double-walled glass vessel containing 1.5 L MMB and 20 mM lactate. Bioreactor dilution rates were controlled to maintain substrate limitation. Bioreactors were maintained at one of three different temperatures, 5, 10, and 21 °C, using external water baths (Neslab, Thermo Fisher Scientific). Chemostat conditions were maintained by controlling pH (7.5) and temperature (5, 10 and 20 °C). Dissolved oxygen concentrations were monitored. Bioreactors were stirred continuously at 50 rpm at an air flow rate of 1 mL min^{-1} unless otherwise described. Each bioreactor contained 10 samples of graphite carbon felt (CF) (3/8-in diameter) impaled on a section of stainless steel tubing connected to a rubber stopper at the top of the bioreactor; flanking each CF was a small length of silicon tubing to act as a spacer. All CF were kept submerged in the bioreactor culture to allow biofilm growth to develop. This design allowed for aseptic removal of individual carbon samples without disturbing the biofilm growth on subsequent pieces. A similar series of experiments were applied to glassy carbon (GC) coupons in batch cultures. Bioreactors were maintained for >7 d. Regular samples were removed from the bioreactors to monitor OD_{600} and cell counts. Culture samples were clarified by filtration (0.2 μm). The concentration of extracellular riboflavin was measured using a 96-well fluorescent plate reader (FlexStation 3; Molecular Devices, Sunnyvale, CA) with an excitation wavelength of 440 nm and observed fluorescence measured at 520 nm. Riboflavin concentrations are reported as the mean of 10 replicate samples and correlated to a standard curve (in the range 25 nM to 1 mM). Lactate concentration was monitored in sample supernatants by high-pressure liquid chromatography (HPLC) (Agilent 1100 HPLC; Agilent Technologies, Santa Clara, CA), equipped with a Phenomenex Rezex 8% organic acid column and by comparison to known standards.

2.2.2. Silica Encapsulation

S. frigidimarina cells were removed from the bioreactor, washed (three times) and resuspended in MMB to an OD_{600} ~5 (equivalent to $9.4 \times 10^9 \pm 2.83 \times 10^8$ CFU mL^{-1}). *S. frigidimarina*–carbon felt anodes (Sf-CF) were prepared from CF wired with a length of titanium wire as described previously [18, 19]. The electrode material was sterilized prior to use and positioned in the center well of a glass petri dish, fabricated to fit the electrode. Washed bacterial cells (5 mL) were applied to the felt electrode to thoroughly wet the material. Tetramethyl orthosilicate (TMOS; 1 mL) was deposited in the outer ring of the glass petri and incubated at 37 °C for approximately 45 min, until the electrode exhibited a white sheen of silica. The TMOS precursor hydrolyzes upon contact with the liquid medium, forming silica that effectively traps the washed cells onto the electrode surface [18] (Si–Sf-CF). Following biofilm development, the electrodes were visualized by scanning electron microscopy (SEM) and also used in electrochemical characterization experiments and MFC testing.

2.2.3. Electrochemical Characterization

Electrochemical measurements were performed with a potentiostat (Versastat 3, Princeton Applied Research; Oak Ridge, TN) and the associated software. All electrochemical

measurements are reported *vs.* Ag/AgCl throughout. Biofilm characterization was carried out via differential pulse voltammetry (DPV) and cyclic voltammetry (CV). CF were removed from the bioreactor, and a 3-mg section removed with a cork borer, placed onto a GC electrode (Metrohm USA, Riverview, FL) and secured with a fabricated Teflon® cap. The GC surface was prepared by polishing with Gamma Micropolish II, deagglomerated alumina, 0.05 μm (Buehler, Lake Bluff, IL) and polishing cloth (TexMet® Buehler). The polish was removed by rinsing with water followed by sonicating in denatured ethanol for 2 min to remove adsorbed alumina particles. The working electrode was placed in an electrochemical chamber (50-mL European five-neck flask with three 14/20 fittings and two #7 threads; Ace Glass, Vineland, NJ) containing 50 mL of MMB, with a platinum rod counter electrode and Ag/AgCl (3 M KCl) reference electrode. Dissolved O_2 was purged from the electrochemical chamber by sparging the MMB with N_2 for 15 min before electrochemical measurements. DPV parameters were as follows: E_i 0 V, E_f -0.7 V (for riboflavin controls) and E_i 0.6 V, E_f -0.7 V (for biofilm characterization), pulse height 50 mV, pulse width 300 ms, step height 2 mV, step width 500 ms, and scan rate 4 mV s^{-1}. CV scan rate was 1 mV s^{-1} and dissolved O_2 was removed from MMB during all CV scans by bubbling with N_2.

2.2.4. MFC Fabrication and Testing

Flow-through MFCs were assembled as described previously [18], by placing the *S. frigidimarina* functionalized anodes in the base of a plastic funnel (55-mm diameter) and over-laying the anode with a polycarbonate membrane (0.2-mm pore size) as separator. A CF cathode was placed on top and sterile MMB with lactate (20 mM) was used as the gravity-fed electrolyte. Open circuit electrode voltage (OCV) was measured using a Personal Daq/54 (IOtech, Cleveland, OH). Polarization potentials were measured on a VersaSTAT 3 potentiostat (Princeton Applied Research) by varying potential and recording steady-state current values. Power was calculated using Ohm's law and normalized based on a geometric surface area of 21 cm^2.

2.2.5. Scanning Electron Microscopy

Materials were prepared for SEM by soaking for 1 h in 0.1 M cacodylate buffer containing 2.5% glutaraldehyde and then increasing concentrations of ethanol in water for 10 min each (50, 70, 80, 90, 100%). The samples were preserved by critical point drying (Tousimis®, Rockville, MD) and coated with gold using a Denton V sputter-coater (Denton Vacuum, LLC, Moorestown, NJ) according to the manufacturer's instructions [20, 21]. SEM imaging was performed using the secondary electron detector of a Hitachi model S-2600N scanning electron microscope (Hitachi High Technologies America, Inc., Pleasanton, CA).

2.3. Results and Discussion

2.3.1. Growth Characteristics of *S. frigidimarina*

One of the advantages of using psychrophilic organisms such as *S. frigidimarina* is the ability to grow and retain viability at a wide range of temperatures (Figure 1). Growth is clearly accelerated at 20 °C, but high culture density is observed at temperatures as low as 5 °C.

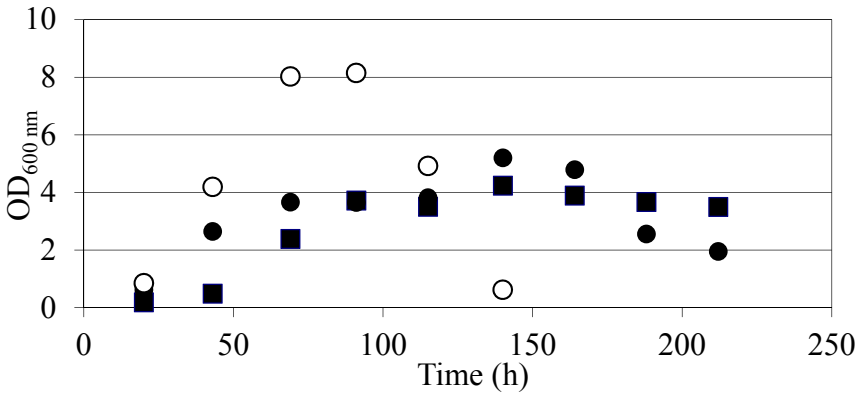

Figure 1. Growth Temperature Profile of *S. frigidimarina*
Growth on 20 mM lactate in MMB; continuous bioreactor
Key: 5 °C (■), 10 °C (●), 20 °C (○)

When incubated with GC electrodes, *S. frigidimarina* initially populates the surface as discreet individual cells. Over a period of several days, the population density increases significantly and a complex three-dimensional biofilm populates the material surface (Figure 2).

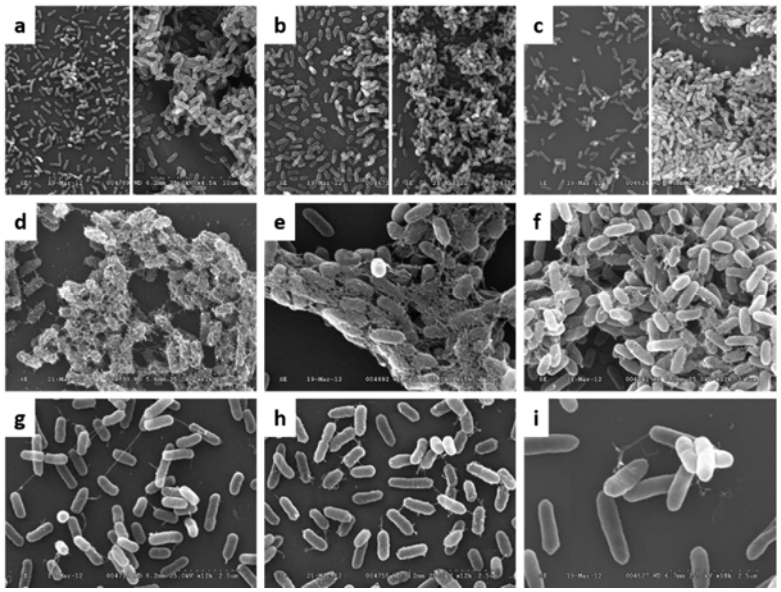

Figure 2. Growth of *S. frigidimarina* on GC
Key: Top row: Growth at 20 °C (a), 10 °C (b) and 5 °C (c) on day 2 (left) and day 6 (right). Extensive exopolysaccharide production and nanowire formation can be observed at all temperatures: 20 °C (d,g) 10 °C (e,h) 5 °C (f,i)

SEM imaging of the cells reveal the formation of extracellular structures consistent with exopolysaccharide (Figure 2). The formation of interconnected cellular pili can also be observed in agreement with other species of *Shewanella* that grow conductive pili termed "nanowires" extending from the cell to anchor to the surface of the electrode [20].

2.3.2. Electrochemical Analysis of *S. frigidimarina*

CF electrodes were removed from the bioreactor and immediately characterized using CV and DPV at 0, 6, 31, 55, 76, and 176 h after inoculation. CV performed at 0 h in MMB confirmed that Faradaic processes were not observed in the absence of microbial growth, although residual oxygen reduction at potentials below -100 mV generated a modest cathodic current. Six h after inoculation, evidence of biofilm formation was observed due to an increase in capacitance during CV (not shown). However, electrodes retrieved 31 h after inoculation exhibited not only a significant increase in capacitance, but anodic current that increased linearly until +0.4 V and decreased significantly during the return sweep (Figure 3).

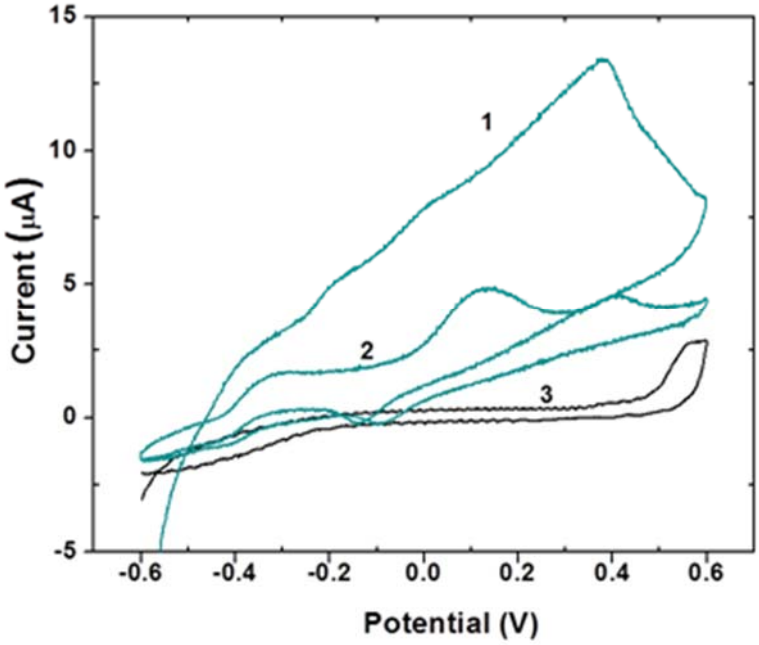

Figure 3. CV of CF Electrodes in MMB 31 h after Inoculation
Key: Scan 1 (1) and scan 2 (2); CV of sterile CF in MMB (3). Scan rate = 1 mV s^{-1}

This indicates that electrochemically active species on (or near) the surface of the electrode were oxidized, but not catalytically replenished. The second scan (performed immediately following the first) exhibited anodic current and indicated possible bioelectrocatalysis associated with biofilm formation. Onset potentials at -0.43 and -0.1 V are tentatively associated with riboflavin oxidation and cytochromes in contact with the surface of the electrode. It has been previously demonstrated that *Shewanella* biofilms grown on conductive surfaces excrete riboflavin. Although the presence of riboflavin is associated with open circuit potentials (OCPs) of ~-0.4 V, it is not clear that the catalytic oxidation of riboflavin is responsible for anodic current. Other mechanisms of extracellular electron transfer have been demonstrated, i.e., interaction of outer membrane cytochromes with the surface of the electrode. In addition, it has been shown that *Shewanella* grow conductive "nanowires"/pili that extend from the cell body and anchor to the

surface of the electrode. Therefore, if one is to construct high-current-density microbial anodes, the mechanism responsible for anodic current production should be elucidated. Given the difficulty resolving redox peaks associated with riboflavin using CV, DPV was performed in abiotic conditions on CF in MMB before and after the addition of riboflavin (Figure 4).

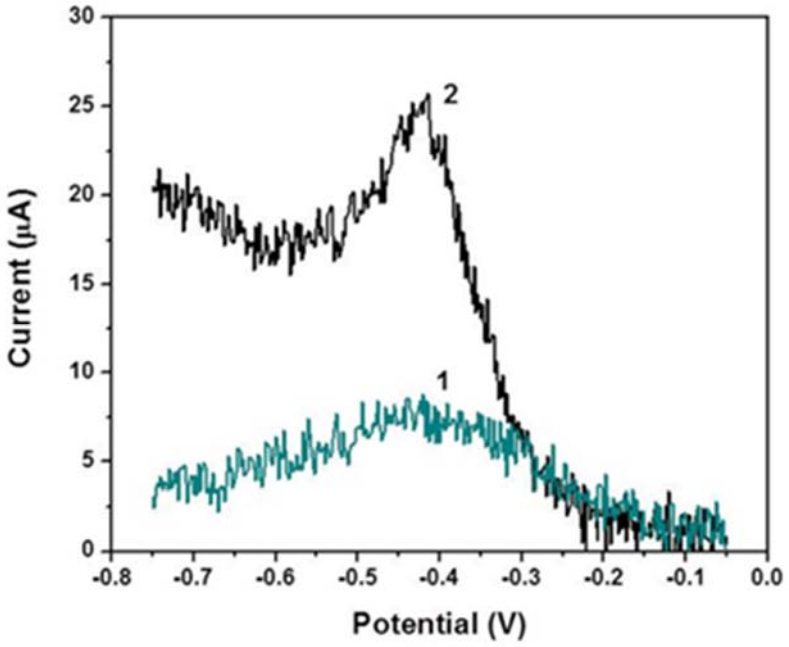

Figure 4. DPV of Sterile CF Electrodes in MMB before (1) and Immediately after (2) Addition of 53 µM Riboflavin

Before the riboflavin addition, a modest peak was observed at -0.42 V; this peak is tentatively associated with B vitamins in the MMB. After the addition of riboflavin, DPV scans revealed a peak at -0.419 ± 0.005 V; $n = 3$. DPV scans performed on CF 31 h after inoculation revealed a comparable peak at ~-0.4 V; as a result this peak is assumed to be associated with riboflavin, however, other analytical methods are needed to confirm the identity of the redox molecule(s). Interestingly, riboflavin was not detected by HPLC in cell extracts. DPV scans performed on CF 55 and 76 h after inoculation revealed peak potentials between -0.30 V and -0.10 V (Figure 5). CV also revealed a quasi-reversible process in a similar potential range (Figure 6).

Riboflavin production was confirmed by CV where distinct oxidation and reduction peaks were observed at -0.45 V vs. Ag/AgCl in agreement with riboflavin standards. As no exogenous riboflavin is added to the system, the redox-active flavin is clearly synthesized by the bacterial biofilm as an endogenous metabolite that is capable of reducing the electrode under electrode polarization. Previous work with *S. frigidimarina* in MMB, however, reported that soluble cyto-chromes were detected in cellular extracts obtained from MFC anodes and could dominate the electron transfer mechanisms [22]; however, this study produced no evidence for that scenario.

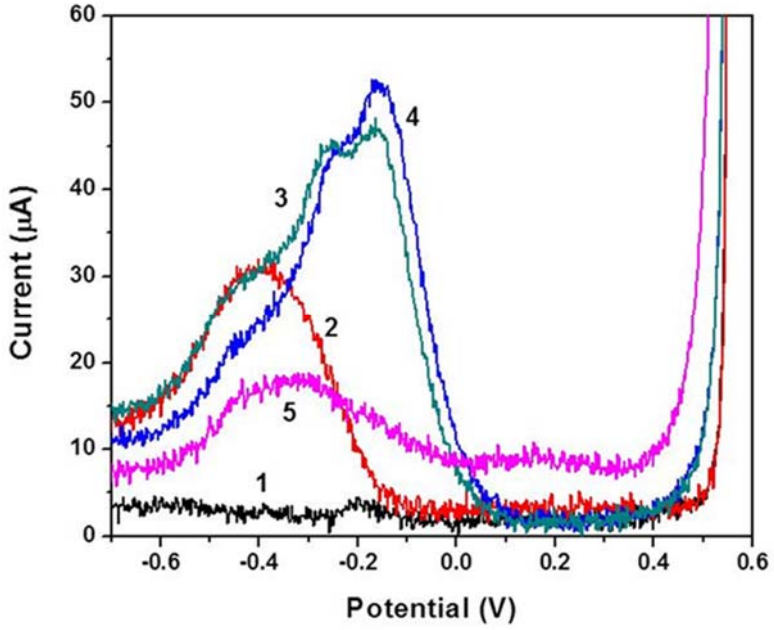

Figure 5. DPV of CF Electrodes Colonized by *S. frigidimarina* in MMB
Key: CF electrodes were submerged in chemostat prior to inoculation and removed for electrochemical analysis. CF electrode tested 6 h (1), 31 h (2), 55 h (3), 76 h (4), and 172 h (5) after inoculation

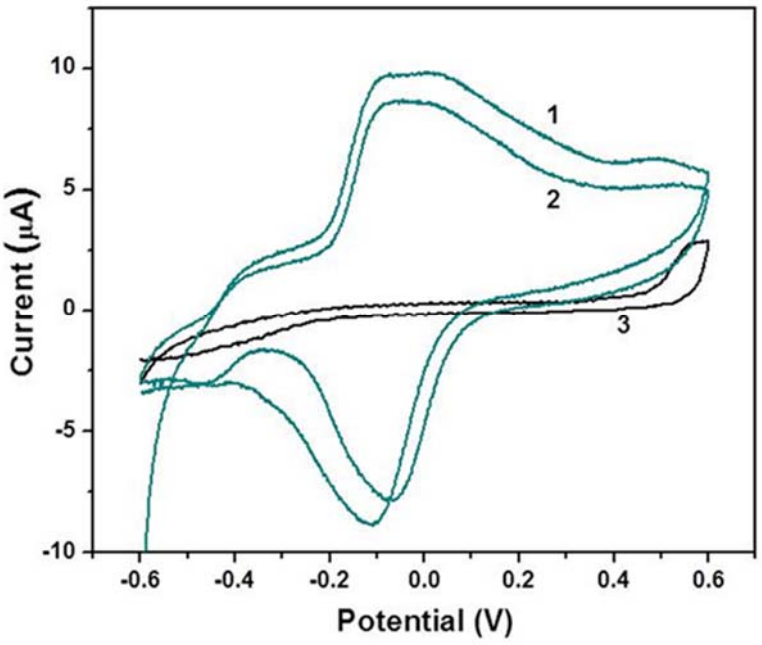

Figure 6. CV of CF Electrodes in MMB 55 h after Inoculation
Key: Scan 1 (1) and scan 2 (2); CV of sterile CF in MMB (3)

2.3.3. Effect of Temperature on Power Output

A series of MFCs were established with *S. frigidimarina* on CF anodes by simple physisorption (Sf-CF) or by using a method for silica-immobilization demonstrated previously (Si–Sf-CF) [13]. The resulting Si–Sf-CF anodes demonstrate similar current density and power density to Sf-CF (Table 1), but the reproducibility of the Si–Sf-CF over duplicate preparations was significantly improved (Figure 7).

Table 1. OCV and Maximum Power Density for *S. frigidimarina* Anodes

Anode preparation	OCV (V)	OCV 10 kΩ load (V)	Maximum power density (μW/cm^2)
Sf-CF	0.39 ± 0.0010	0.169 ± 0.0012	0.074 ± 0.040, *n*=5
Si–Sf-CF	0.38 ± 0.0005	0.167 ± 0.0015	0.068 ± 0.014, *n*=5

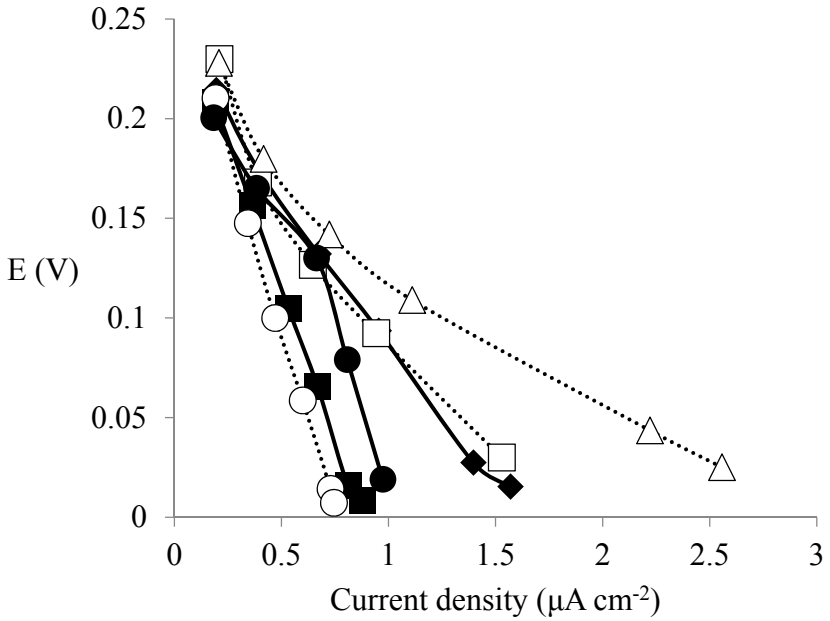

Figure 7. Potentiostatic Polarization Curves for Sf-CF and Si–Sf-CF Anodes
Key: Silica-immobilized (solid shapes); physisorbed (hollow shapes)

In the initial MFC preparations, *S. frigidimarina* was cultured at 4 °C and operated at room temperature 27 °C (Table 1 and Figure 7). To determine the effect of temperature (both growth and operating temperature), a series of MFCs were prepared in which *S. frigidimarina* was grown at 4, 11 or 27 °C. The resulting MFCs were then tested at the same range of operating temperatures (Table 2).

MFCs prepared from Si–Sf-CF grown, and operated, at 4 °C did not produce measurable currents despite numerous attempts. Si–Sf-CF prepared from cells grown at 4 °C did, however, produce measureable power output when the operating temperature was elevated to 11 or 27 °C. Growth and operation at 11 °C resulted in power density and current density that was ~50% of

Table 2. Electrochemical Characteristics of Si-Sf-CF Microbial Fuel Cells at Various Operating Temperatures

Growth temp (°C)	MFC temp (°C)	OCV (V)	Max current density μA/cm^3	Max power density μW/cm^3
4	4	0	0	0
4	11	0.127 ± 0.102	unstable under load	unstable under load
4	27	0.370 ± 0.006	1.16 ± 0.29 (*n*=2)	0.09 ± 0.04 (*n*=2)
11	11	0.214 ± 0.006	0.88 ± 0.54 (*n*=3)	0.04 ± 0.03 (*n*=3)
27	4	0.402 ± 0.012	1.12 ± 0.24 (*n*=2)	0.11 ± 0.05 (*n*=2)
27	11	0.411 ± 0.012	1.21 ± 0.72 (*n*=4)	0.12 ± 0.08 (*n*=4)
27	27	0.428 ± 0.003	1.45 ± 0.82 (*n*=6)	0.14 ± 0.06 (*n*=6)

maximum output (based on the configurations reported herein). Notably, Si–Sf-CF prepared from cells grown at 27 °C produced comparable maximum current and power density irrespective of the operating temperatures (ranging from 4–27 °C) (Table 2). Loss in performance was noted, however, if the temperature was increased to 37 °C (data not shown).

2.4. Conclusions

For field applications, MFCs must be able to tolerate variations in environmental temperature. The potential power output and operating range was investigated for *S. frigidimarina* as an anodic catalyst within MFCs. MFCs were established with immobilized biofilms pre-conditioned to varying temperatures and the effect on power output was determined. The maximum power density of ~0.14 μW/cm^3 was achieved at all operating temperatures and regardless of growth at 4 °C or 27 °C, suggesting that electrochemical activity of *S. frigidimarina* is independent of temperature. These results demonstrate that MFCs can effectively be operated at a wide range of environmental temperatures. Further experiments are needed to more precisely determine the range of growth conditions of *S. frigidimarina*.

3. Twisted Morphology of *Shewanella japonica*

3.1. Introduction

Members of the *Shewanella* genus are a diverse group of marine γ-proteobacteria and are noted for their wide metabolic spectrum and ability to survive in diverse environments [23]. *S. oneidensis*, for example, has been used in a wide variety of biotechnology applications, from detoxification of heavy metals and bioremediation of organic pollutants to generation of electricity in MFCs [18, 24–28]. *S. oneidensis* can use a wide variety of metals as electron acceptors, and as a result, the organism has also been studied for the ability to attach and develop biofilms on metal surfaces [29–33].

In this study, we examined cell attachment and growth of the lesser-known *Shewanella* species *S. japonica* on aluminum surfaces. The species was only recently discovered, in 2001 [34], and to date, there have been only a few studies of the growth characteristics of this marine microorganism, though its utility in MFCs has recently been reported [35]. Due to its ability to utilize extracellular electron acceptors and transfer electrons to a conductive surface, *S. japonica* was also chosen as a candidate for analyzing microbe-induced corrosion on bare and painted aluminum surfaces. Herein, a recirculating, continuous-flow bioreactor was constructed to allow controlled exposure of aluminum coupons to *S. japonica* cultures. The bioreactor construction allows for uniform flow of bacteria over the entire coupon surface and permits removal of a subset of coupons for analysis without disrupting the overall conditions. Microscopy of the coupons and biofilms showed no appreciable change to the coupon surfaces but led to the discovery of a very unusual twisted cellular morphology for *S. japonica* cells when attached to the surface.

3.2. Methods, Assumptions, and Procedures

3.2.1. Sample Materials and Bioreactor Design

All silicone tubing was obtained from Cole–Parmer Instrument Company (Vernon Hills, IL). Sample surfaces were aluminum 7075 coupons (10 × 20 mm) of a thickness 0.8~0.9 mm. Coupons were either bare or coated with polyurethane paint. The bioreactor design provided a uniform flow rate over all coupon surfaces simultaneously within a closed, recirculating batch culture (approximately 1.5 L total volume; Figure 8). A culture reservoir (250 mL) was pumped into a glass manifold (560 mL) through two lower inlets. Six upper outlets were connected to six glass tubes (12 × 200 mm). Each glass tube held up to 12 sample coupons. The tubes were then connected to a second glass manifold at six upper inlets. The culture medium exited the second manifold through two lower glass ports and returned to the culture reservoir. Silicone tubing was used throughout to connect ports and glass tubes. Peristaltic pumping was supplied by a Dynamax RP-1 pump (Rainin Instruments, LLC, Oakland, CA) using two lengths of silicone tubing (2.8 mm ID). The manifolds allowed for continuous and equal flow through all tubes at approximately 5 mL min^{-1}. A 21-gauge, 38.1-mm needle (Becton, Dickinson & Co.) fitted with a cellulose acetate syringe filter (0.2 μm pore size; Nalgene, Thermo Fisher Scientific, Rochester, NY) allowed equalization of air pressure between bioreactor and atmosphere. A sample port was located in the reservoir for removal of culture fluid for analysis.

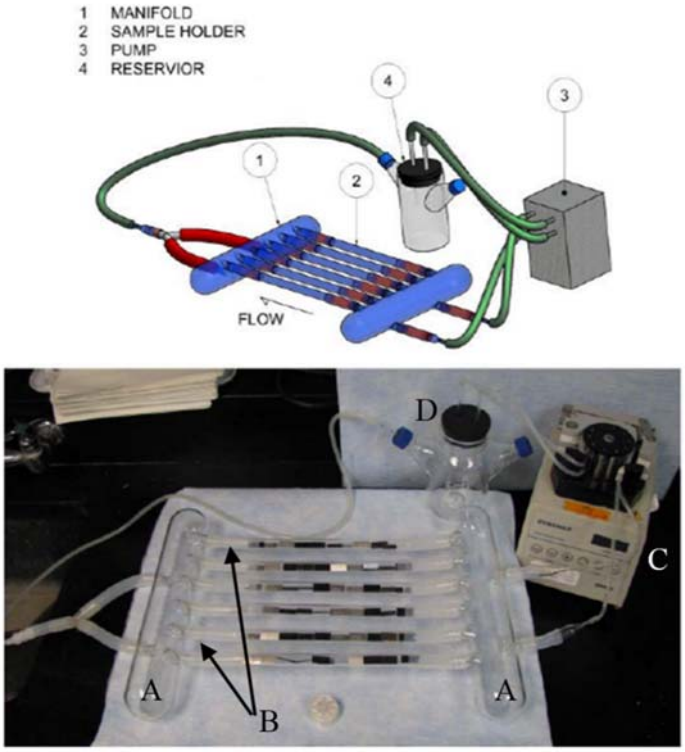

Figure 8. Schematic (top) and Image (bottom) of Coupon Bioreactor
Key: The bioreactor comprises two manifolds (A), six sample holders (B), a pump (C), and a culture medium reservoir (D)

3.2.2. Bacterial Culture Conditions

All chemicals were obtained from Sigma–Aldrich unless noted otherwise. Culture medium consisted of Difco Marine Broth (MB) 2216 (Becton, Dickinson and Co.), prepared as directed and diluted 1:1 with water. Sufficient NaCl was then added to bring the final concentration up to 19.45 g L^{-1}. Defined culture medium (DM, pH 7.6) was prepared with identical inorganic ingredients and concentrations as MB (g L^{-1}): NaCl, 19.45; $MgCl_2$, 5.9; $MgSO_4$, 3.24; $CaCl_2$, 1.8; KCl, 0.55; Na_2CO_3, 0.16; KBr, 0.08; $SrCl_2$, 0.034; H_3BO_3, 0.022; Na_2SiO_3, 0.004; NaF, 0.0024; NH_4NO_3, 0.0016; Na_2HPO_4, 0.008. The DM was supplemented with Wolfe's mineral and vitamin solutions [20]. Peptone and yeast extract were omitted and replaced with high-purity agarose (0.2%, final concentration) as the carbon source (SeaKem Gold, FMC Bioproducts, Rockland, ME).

Two bioreactor cultures containing DM and one separate bioreactor culture containing MB were incubated at room temperature, each over the course of 14 d. Each bioreactor was inoculated with a 10-mL overnight culture of *S. japonica* (ATCC strain BAA-316,) grown in MB. Growth in DM was monitored by serial dilution plate counts to solid MB containing 1.5% agar and enumerating colony-forming units (CFU mL^{-1}) after incubation at room temperature for 36 h. Growth in dilute MB was monitored spectrophotometrically by measuring optical density at 600 nm (Cary Instruments, Agilent Technologies). Culture purity in all bioreactors was monitored daily by plating serial dilutions on three different types of solid media (MB, Luria broth, and DM; all containing 1.5% agarose) and inspecting colony morphology.

3.2.3. Sample Preparation and Microscopy

At specific time intervals, one glass tube containing the aluminum coupons was removed from the bioreactor at the silicone tubing connectors and replaced with an empty sterile glass tube. Coupons were then removed from the tubes with forceps, washed in PBS [36], and processed for SEM analysis using methods previously stated in Section 2.2.5. An average of six coupons were prepared for each time interval.

3.3. Results and Discussion

3.3.1. Growth and Morphology of *S. japonica* Cells on Aluminum Surfaces Grown in DM with Agarose

Initial cell counts showed all bioreactor cultures in DM contained 10^6 –10^7 cells mL^{-1}. Growth was observed for up to 5 d, when planktonic cell counts increased ~tenfold to 10^7–10^8 cells mL^{-1}. The number of viable planktonic cells then slowly declined to 10^6 –10^7 cells mL^{-1} for the remainder of the 14 d (Figure 9). The decrease in cell viability was not due to a shortage of carbon source, as the agarose formed a semi-molten state in the bioreactor and was observed throughout the entire course of the experiment.

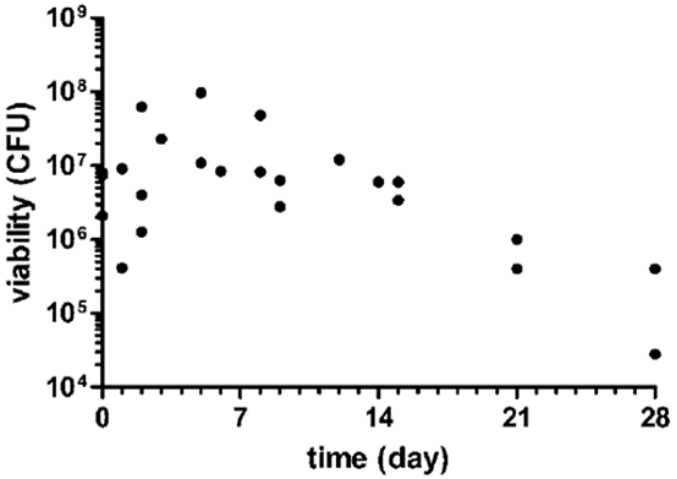

Figure 9. Growth of *S. japonica* Cultures (CFU mL^{-1}), *n*=3

Figure 10 shows representative SEM images of *S. japonica* cells attached to coupons removed after 2-, 7-, and 14-d incubation in the bioreactor (additional images are shown in the appendix). After 2 d incubation, most cells attached to surfaces were rod-shaped and divided to form chains (Figure 10a–c). Significantly elongated cells were present, but most cells were straight rods or slightly curved. In a few cases, the cells were curled and began to form spirals. The intense electron-scattering material (white material) imaged on coupons was precipitated salts that formed between the aluminum and inorganic ions from the medium. After 7 d incubation, cells continued to lengthen, mostly as longer curved rods, but highly twisted cells were also observed (Figure 10d–f). Spiral growth was sporadic; cells elongated as straight rods and then would inexplicably twist into variably loose or tight spirals. All spiraling cells were left-handed helices, although in one case, helix direction appeared to have switched in a single cell or chain of cells (Figure 10h). In addition, a morphological feature known as nanowires was observed after 14 d incubation (Figure 10i). These pili-like appendages are different from flagella and have been implicated in extracellular electron transfer [20].

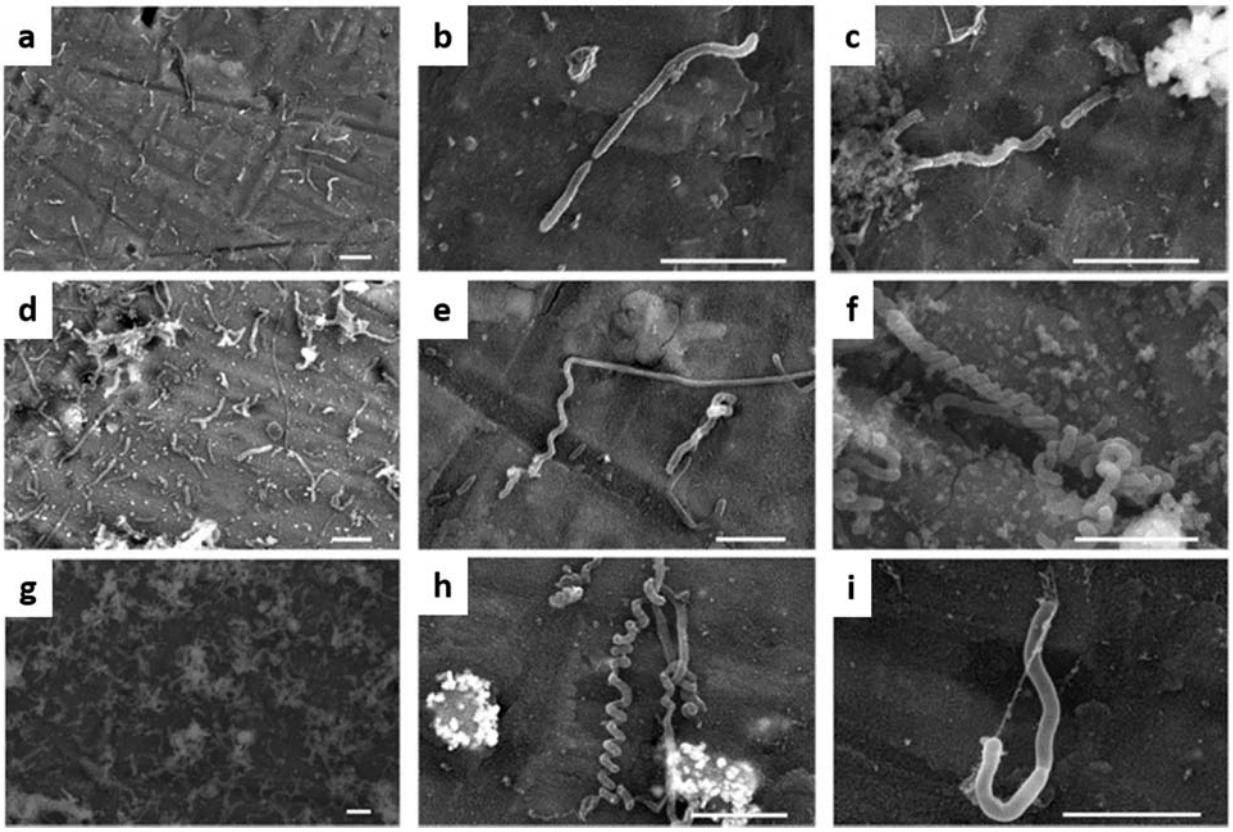

Figure 10. SEM Images of *S. japonica* Cells on Al Coupons
Key: After 2 d (top row), 7 d (middle row), and 14 d (bottom row) incubation in the coupon bioreactor. Scale bars = 5 µm.

3.3.2. Growth and Cellular Morphology of *S. japonica* Grown on Aluminum Surfaces Grown in MB

S. japonica cultures grown in MB were inoculated and operated under identical conditions to the bioreactor cultures with DM. Planktonic cells grew exponentially for the first 24 h and appeared to enter starvation and stationary phase after 2 d. Coupons were removed from the bioreactors after incubation for 1, 2, 3, 6, 7, and 14 d. During exponential growth, cells grown in MB were shorter and wider than cells grown in DM (Figure 10). The cells divided rapidly during the first and second days of incubation. Numerous nanowires were present and some cells exhibited a cellular sheath. Starting at day 3, however, some cells began to take on the longer, more slender likeness of those grown in DM, though short rods were still common. This trend continued to day 14 and more cells were imaged as elongated rods. At the end of the incubation period, cellular morphology was very similar to those observed in DM cultures, except spiral cells were not observed (additional images are found in the appendix).

Original reports describe *S. japonica* as a polar-flagellated short rod 1–2 µm in length and 0.6–0.8 µm in diameter when grown with conventional microbiological practices [34]. A more recent account of *S. japonica* grown as biofilms for MFCs described the same rod-shaped cells and the appearance of multiple flagella and pili-type (nanowire) structures around the cell body [35]. In addition, a sheath-like structure was also observed surrounding cells. In the previous studies,

cells were grown on a rich, undefined nutrient broth similar to MB and a similar cellular morphology was also observed in the MB bioreactor cultures during logarithmic growth. In all cultures, there was no apparent difference in cell number or morphology on either bare or painted coupon surfaces. The extended rod morphology has not been previously reported for *S. japonica,* although cell elongation in late lag phase culture or under nutrient-limited environments is a commonly reported phenomenon for many microorganisms [37]. This type of cell growth is a beneficial response to the lack of one or more nutrients; the change in shape allows for more proficient uptake of nutrients by increasing the surface area of the cell membrane, while keeping the surface-to-volume ratio of the cell relatively unchanged [37]. As an added benefit to biofilm formation, lengthening increases cell surface in contact with a surface. In bioreactor cultures containing MB, cell elongation was observed when cultures entered stationary phase. Under DM conditions, agarose was in excess throughout the incubation period, but the bioavailability of low-molecular-weight agarose oligomers (*e.g.,* agarobiose) that are readily utilized by *S. japonica* were likely metabolized in the first days of incubation, along with any residual nutrients that transferred with the inoculum culture. After consumption of these carbon sources, the obstinate breakdown of larger agarose polymers slowed growth and most likely resulted in the substrate-limited conditions that induced cell elongation.

Whereas filamentous growth is not surprising, the twisted morphology of *S. japonica* cells is unique and has not been previously reported for any *Shewanella* species. Our understanding of spiral cell formation does not readily explain the morphology observed with *S. japonica* cells. Many marine microorganisms are vibroid and the extension of the cellular fibers that maintain the curvature of the cell during elongation will result in regular spirals [37, 38]. Also, many polar flagellated bacteria (*e.g.*, *Spirochaete* sp.) have an axial filament that runs the length of the cell—unequal lengthening of this axial filament at this ends during cell elongation may cause a normally short, polar-flagellated rod to become twisted. This does not appear to be true in either case, because *S. japonica* cells do not appear to be typically vibroid and cells elongate as straight rods, then inexplicitly twist into tight and loose spirals. Yet, all spirals are left-handed helices, which suggest a structural relationship between growth and cytoskeletal components. The spiral reversal within one cell or chain of cells is likely not biotic and is a prime example of perversion—a bifurcation into two opposite-handed helices caused by physical tension on a filament with intrinsic curvature or, in simpler terms, the classic kink that forms in a telephone cord when it is repeatedly extended and recoiled [39].

Spirochetes, such as *Treponema,* and other intestinal microorganisms such as *Helicobacter pylori*, exploit their helical morphology to swim efficiently through viscous fluids found in the gastrointestinal tract [37]. Similar viscous environments are found in marine environments, such as polymer slime layers and biofilms secreted by plants, algae, mollusks, and other bacteria. As *S. japonica* cells are motile and agarose is a marine plant polysaccharide, it is possible that growth in the semi-molten agarose medium induces spiral formation for more efficient mobility. It is unlikely that induction of spiral growth is caused by a change in the surrounding viscosity. Typically, nutrient composition dictates metabolism-dependent, morphological changes in bacterial cell shape. Hence, spiral morphology may be induced by the viscous environment's nutrients and not by the dense aqueous environment itself. The helical-shaped, saccharolytic marine and freshwater spirochetes are a prime example of this structure–function relationship. Yet, to our knowledge, an association between shape, metabolic requirements, and

environmental density has not been discovered in the spirochetes. Alternatively, studies in motility and high-viscosity environments (*e.g.*, mucus) has been completed using oral- and intestinal-associated spirochetes, and analogous studies using spirochetes are warranted to identify if this association exists in marine and freshwater environments.

3.4. Conclusions

The constructed bioreactor system presented herein facilitates the thorough analysis of cell attachment and biofilm formation on sample surfaces, and analysis of replicates at numerous time-points within one experimental setup. We were able to obtain evidence of unique *S. japonica* cell morphology on coupon surfaces over the course of three bioreactor experiments. Further studies are necessary to determine not only the reason for the elongation and spiraling pattern seen in these cells, but also to determine if other cells behave in a similar manner when cultured in this particular way.

4. LIST OF SYMBOLS, ABBREVIATIONS, AND ACRONYMS

CF	graphite carbon felt
CFU	colony-forming units
CV	cyclic voltammetry
DM	defined culture medium
DPV	differential pulse voltammetry
GC	glassy carbon
HPLC	high-pressure liquid chromatography
MB	marine broth
MFC	microbial fuel cell
MMB	modified marine broth
OCP	open circuit potential
OCV	open circuit voltage
OD	optical density
PBS	phosphate buffered saline
SEM	scanning electron microscopy
Sf	*S. frigidimarina*
Sf-CF	*S. frigidimarina* on a carbon electrode
Si–Sf-CF	silica-immobilized Sf-C
TMOS	tetramethyl orthosilicate

5. REFERENCES

1. Liu H, Logan B. 2004. Electricity generation using an air-cathode single chamber microbial fuel cell in the presence and absence of a proton exchange membrane. *Environ Sci Technol*. **38**(14): 4040–4046.
2. Liu H, Ramnarayanan R, Logan B. 2004. Production of electricity during wastewater treatment using a single chamber microbial fuel cell. *Environ Sci Technol*. **38**(7): 2281–2285.
3. Min B, Logan B. 2004. Continuous electricity generation from domestic wastewater and organic substrates in a flat plate microbial fuel cell. *Environ Sci Technol*. **38**(21): 5809–5814.
4. Heilmann J, Logan B. 2006. Production of electricity from proteins using a microbial fuel cell. *Water Environ Res*. **78**(5): 531–7.
5. Wagner R, Porter-Gill S, Logan B. 2012. Immobilization of anode-attached microbes in a microbial fuel cell. *AMB Express*. **2**(2): 1–6.
6. Ren L, Ahn Y, Logan B. 2014. A two-stage microbial fuel cell and anaerobic fluidized bed membrane bioreactor (MFC-AFMBR) system for effective domestic wastewater treatment. *Environ Sci Technol*. **48**(7): 4199–4206.
7. Bowman J, Mccammon S, Nichols D, Skerratt J, Rea S, Nichols P, Mcmeekin T. 1997. *Shewanella gelidimarina* sp. nov. and *Shewanella frigidimarina* sp. nov., novel Antarctic species with the ability to produce eicosapentaenoic acid (20:ω3) and grow anaerobically by dissimilatory Fe(III) reduction. *Int J Syst Bacteriol*. **47**(4): 1040–1047.
8. Dobbin P, Butt J, Powell A, Reid G, Richardson D. 1999. Characterization of a flavocytochrome that is induced during the anaerobic respiration of Fe^{3+} by *Shewanella frigidimarina* NCIMB400. *Biochem J*. **342 (Pt 2)**: 439–448.
9. Tsapin A, Vandenberghe I, Nealson K, Scott J, Meyer T, Cusanovich M, Harada E, Kaizu T, Akutsu H, Leys D, Van Beeumen J. 2001. Identification of a small tetraheme cytochrome c and a flavocytochrome c as two of the principal soluble cytochromes c in *Shewanella oneidensis* strain MR1. *Appl Environ Microbiol*. **67**(7): 3236–3244.
10. Turner K, Doherty M, Heering H, Armstrong F, Reid G, Chapman S. 1999. Redox properties of flavocytochrome c3 from *Shewanella frigidimarina* NCIMB400. *Biochemistry*. **38**(11): 3302–3309.
11. Paquete C, Saraiva I, Calcada E, Louro R. 2010. Molecular basis for directional electron transfer. *J Biol Chem*. **285**(14): 10370–10375.
12. Fitzgerald L, Petersen E, Leary D, Nadeau L, Soto C, Ray R, Little B, Ringeisen B, Johnson G, Vora G, Biffinger J. 2013. *Shewanella frigidimarin*a microbial fuel cells and the influence of divalent cations on current output. *Biosens Bioelectron*. **40**(1): 102–109.
13. Behera M, Murthy S, Ghangrekar M. 2011. Effect of operating temperature on performance of microbial fuel cell. *Water Sci Technol*. **64**(4): 917–922.
14. Gong Y, Radachowsky S, Wolf M, Nielsen M, Girguis P, Reimers C. 2011. Benthic microbial fuel cell as direct power source for an acoustic modem and seawater oxygen/temperature sensor system. *Environ Sci Technol*. **45**(11): 5047–5053.
15. Jadhav G, Ghangrekar M. 2009. Performance of microbial fuel cell subjected to variation in pH, temperature, external load and substrate concentration. *Bioresour Technol*. **100**(2): 717–723.

16. Li L, Sun Y, Yuan Z, Kong X, Li Y. 2013. Effect of temperature change on power generation of microbial fuel cell. *Environ Technol*. **34**(13–16): 1929–1934.
17. Min B, Roman O, Angelidaki I. 2008. Importance of temperature and anodic medium composition on microbial fuel cell (MFC) performance. *Biotechnol Lett*. **30**(7): 1213–1218.
18. Luckarift H, Sizemore R, Roy J, Lau C, Gupta G, Atanassov P, Johnson G. 2010. Standardized microbial fuel cell anodes of silica-immobilized *Shewanella oneidensis*. *Chem Comm*. **46**(33): 6048–6050.
19. Luckarift H, Sizemore S, Farrington K, Fulmer P, Biffinger J, Nadeau L, Johnson G. 2011. Biodegradation of medium chain hydrocarbons by *Acinetobacter venetianus* 2AW immobilized to hair-based adsorbent mats. *Biotechnol Prog*. **27**(6): 1580–1587.
20. Gorby Y, Yanina S, Mclean J, Rosso K, Moyles D, Dohnalkova A, Beveridge T, Chang I, Kim B, Kim K, Culley D, Reed S, Romine M, Saffarini D, Hill E, Shi L, Elias D, Kennedy D, Pinchuk G, Watanabe K, Ishii S, Logan B, Nealson K, Fredrickson J. 2006. Electrically conductive bacterial nanowires produced by *Shewanella oneidensis* strain MR-1 and other microorganisms. *Proc Natl Acad Sci USA*. **103**(30): 11358–11363.
21. Ray R, Lizewski S, Fitzgerald L, Little B, Ringeisen B. 2010. Methods for imaging *Shewanella oneidensis* MR-1 nanofilaments. *J Microbiol Meth*. **82**(2): 187–191.
22. Fitzgerald LA, Petersen ER, Leary DH, Nadeau LJ, Soto CM, Ray RI, Little BJ, Ringeisen BR, Johnson GR, Vora GJ, Biffinger JC. 2013. Shewanella frigidimarina microbial fuel cells and the influence of divalent cations on current output. *Biosens Bioelectron*. **40**(1): 102–9.
23. Kato C, Nogi Y. 2001. Correlation between phylogenetic structure and function: examples from deep-sea *Shewanella*. *FEMS Microbiol Ecol*. **35**: 223–230.
24. Biffinger J, Ribbens M, Ringeisen B, Pietron J, Finkel S, Nealson K. 2009. Characterization of electrochemically active bacteria utilizing a high-throughput voltage-based screening assay. *Biotechnol Bioeng*. **102**(2): 436–444.
25. Biffinger J, Ray R, Little B, Fitzgerald L, Ribbens M, Finkel S, Ringeisen B. 2009. Simultaneous analysis of physiological and electrical output changes in an operating microbial fuel cell with *Shewanella oneidensis*. *Biotechnol Bioeng*. **103**(3): 524–531.
26. Heidelberg J, Paulsen I, Nelson K, Gaidos E, Nelson W, Read T, Eisen J, Seshadri R, Ward N, Methe B, Clayton R, Meyer T, Tsapin A, Scott J, Beanan M, Brinkac L, Daugherty S, Deboy R, Dodson R, Durkin A, Haft D, Kolonay J, Madupu R, Peterson J, Umayam L, White O, Wolf AM, Vamathevan J, Weidman J, Impraim M, Lee K, Berry K, Lee C, Mueller J, Khouri H, Gill J, Utterback T, Mcdonald L, Feldblyum T, Smith H, Venter J, Nealson K, Fraser C. 2002. Genome sequence of the dissimilatory metal ion-reducing bacterium *Shewanella oneidensis*. *Nat Biotechnol*. **20**(11): 1118–23.
27. Lanthier M, Gregory K, Lovley D. 2008. Growth with high planktonic biomass in *Shewanella oneidensis* fuel cells. *FEMS Microbiol Lett*. **278**: 29–35.
28. Payne A, Dichristina T. 2006. A rapid mutant screening technique for detection of technetium [Tc(VII)] reduction-deficient mutants of *Shewanella oneidensis* MR-1. *FEMS Microbiol Lett*. **259**: 282–287.
29. Dawood B. 1998. Corrosion-enhancing potential of *Shewanella putrefaciens* isolated from industrial cooling waters. *J Appl Microbiol*. **84**: 929–936.
30. Kuş E, Nealson K, Mansfeld F. 2007. The effect of different exposure conditions on the biofilm/copper interface. *Corr Sci* **49**: 3421–3427.

31. Mansfeld F. 2007. The interaction of bacteria and metal surfaces. *Electrochim Acta*. **52**: 7670–7680.
32. Goodson W, Wc P, Knight C, Kay M, Lloyd P, *Impact of medium and substrate on growth of Pseudomonas fluorescens biofilms on polyurethane paint*, AFRL, Editor. 2011.
33. Crookes-Goodson W, Mirau P, Bojanowski C, Kay M, Lloyd P, Blankemeir A, Fraser H, Bralow D, Pehrsson P, Russell Jr J, Eby D, Johnson G, *Impact of medium on the development and physiology of Pseudomonas fluorescens biofilms on polyurethane paint*, AFRL, Editor. 2012.
34. Ivanova E, Sawabe T, Gorshkova N, Svetashev V, Mikhailov V, Nicolau D, Christen R. 2001. *Shewanella japonica* sp. nov. *Int J Syst Evol Microbiol* **51**: 1027–1033.
35. Biffinger J, Fitzgerald L, Ray R, Little B, Lizewski S, Petersen E, Ringeisen B, Sanders W, Sheehan P, Pietron J, Baldwin J, Nadeau L, Johnson G, Ribbens M, Finkel S, Nealson K. 2011. The utility of *Shewanella japonica* for microbial fuel cells. *Bioresour Technol*. **102**(1): 290–297.
36. Sambrook J, Fritsch E, Maniatis T, *Molecular Cloning: A Laboratory Manual*, ed. C.S.H. Cold Spring Harbor Laboratory, NY. 1989.
37. Young K. 2006. The selective value of bacterial shape. *Microbiol Molec Biol Rev*. **70**: 660–703.
38. Wolgemuth C, Inclan Y, Quan J, Mukherjee S, Oster G, Koehl M. 2005. How to make a spiral bacterium. *Phys Biol*. **2**: 189–199.
39. Goriely A, Tabor M. 1998. Spontaneous helix hand reversal and tendril perversion in climbing plants. *Phys Rev Lett* **80**: 1564–1567.

APPENDIX: SEM Images of *S. japonica* (Sj) on Aluminum Coupons

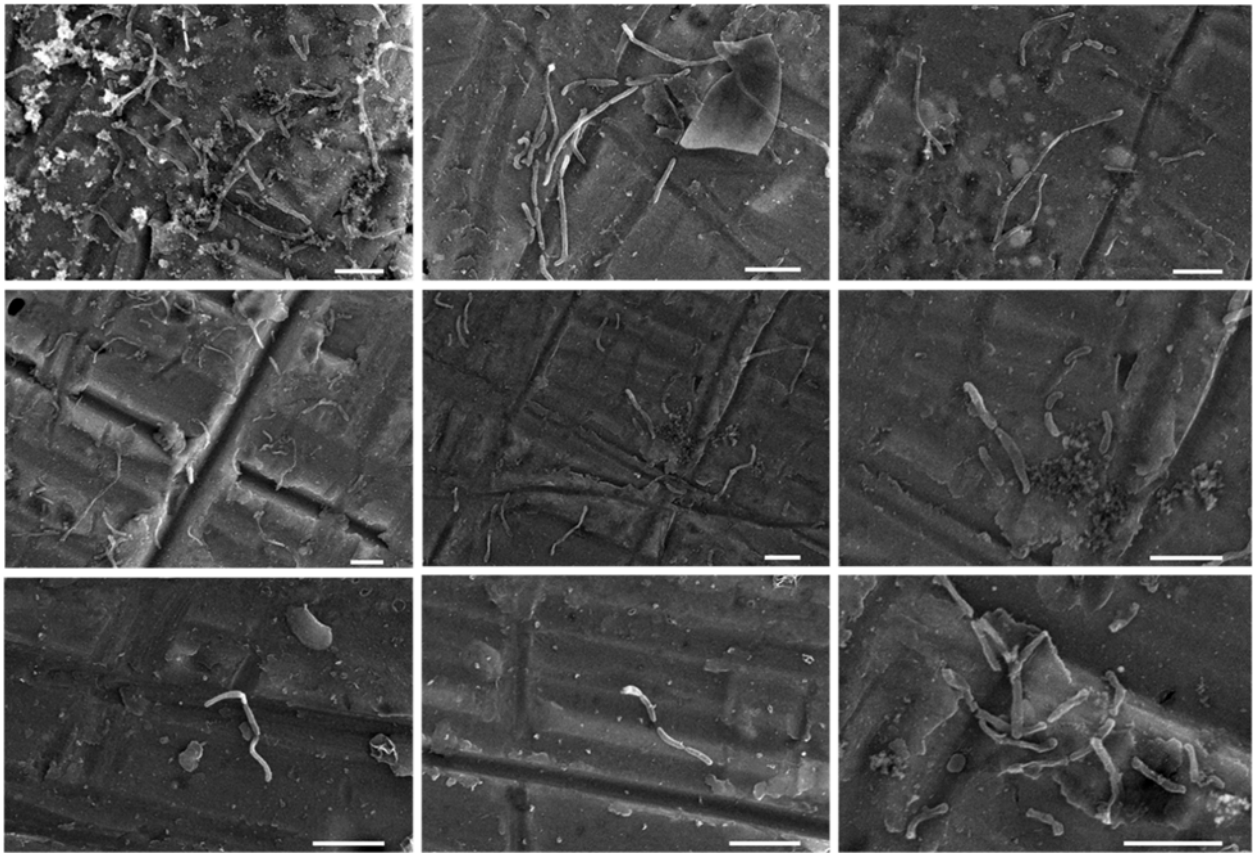

Figure 11. *Shewanella japonica* Cells after 2-d Incubation in Defined Culture Medium with Agarose

All coupons unpainted
Scale bars = 5 µm

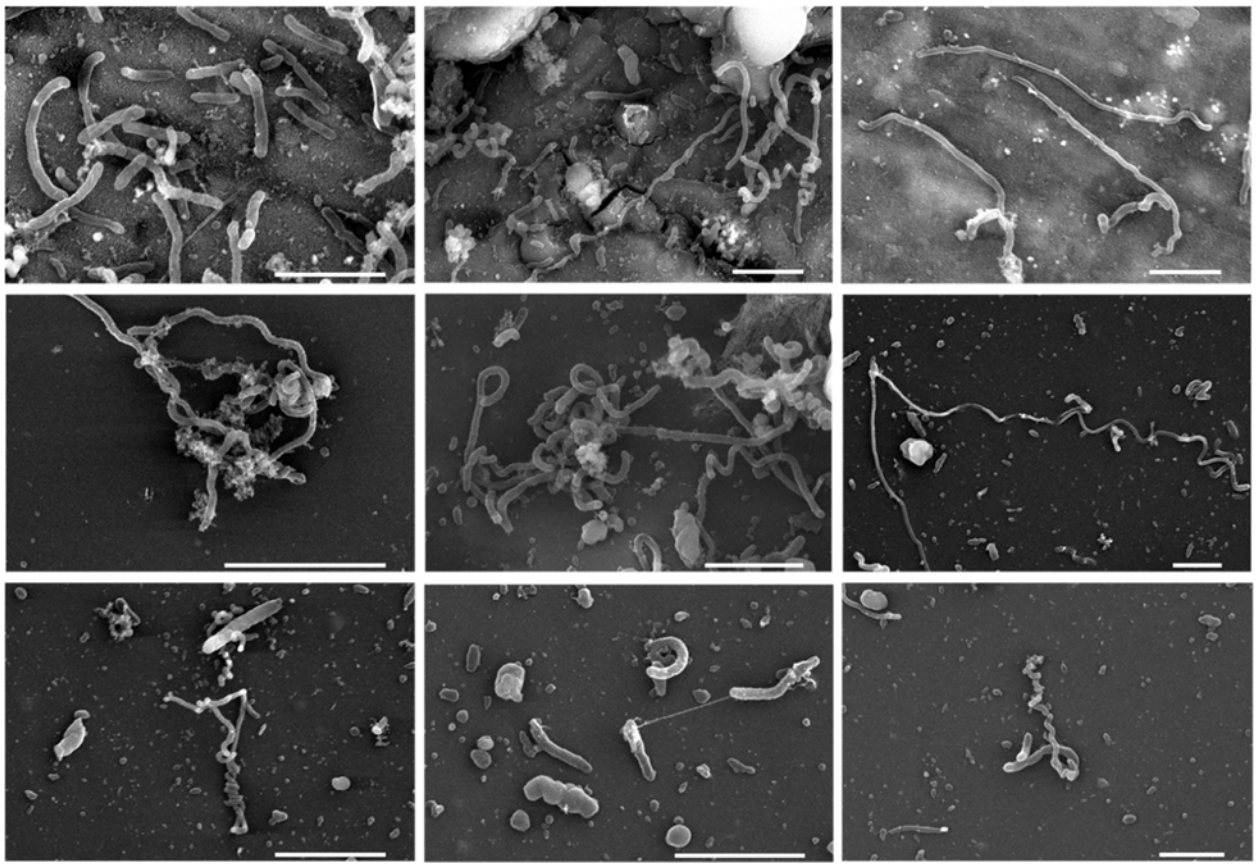

Figure 12. *Shewanella japonica* Cells after 7-d Incubation in Defined Culture Medium with Agarose

Unpainted coupons (top row); coupons coated with polyurethane paint (middle row); coupons coated with polyurethane paint containing carbon black nanoparticles (bottom row)
Scale bars = 5 μm

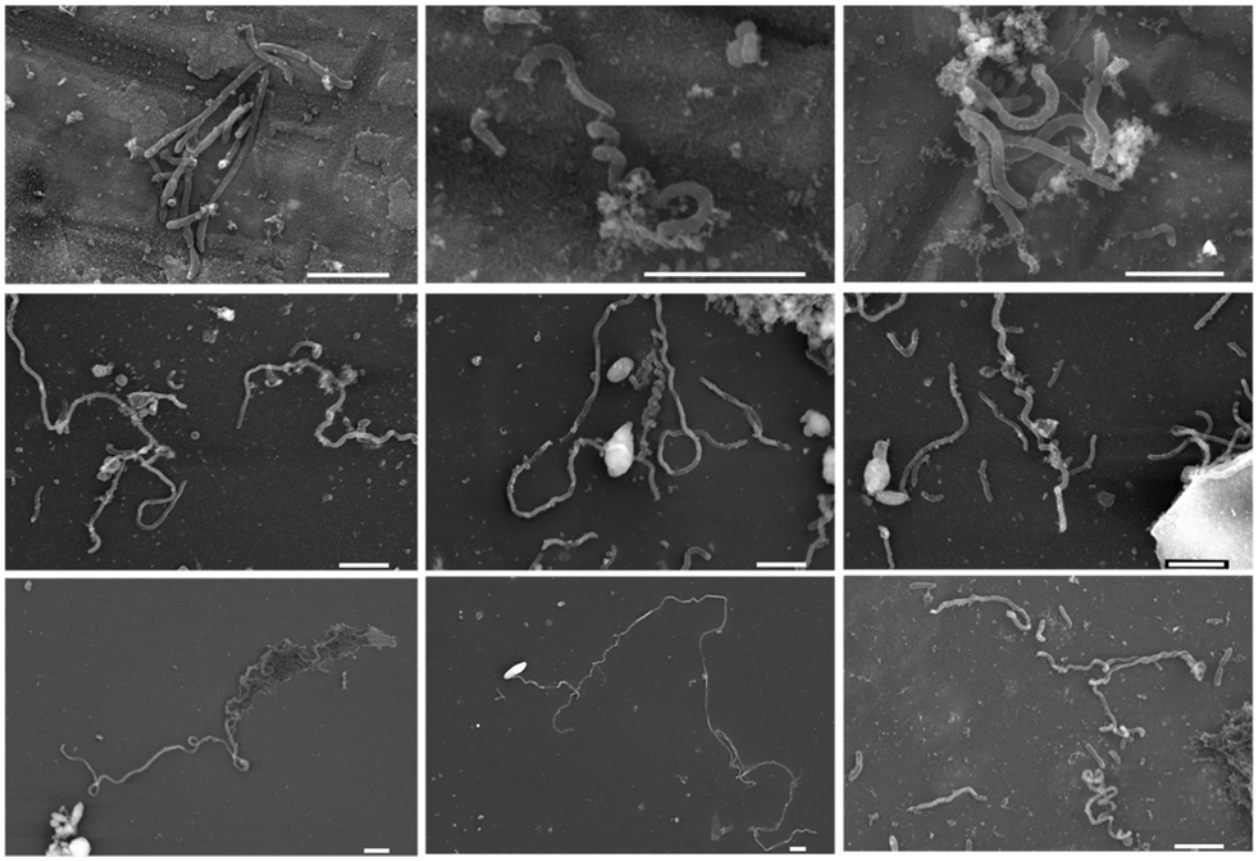

Figure 13. *Shewanella japonica* cells after 14-d Incubation in Defined Culture Medium with Agarose

Unpainted coupons (top row); coupons coated with polyurethane paint (middle row); coupons coated with polyurethane paint containing carbon black nanoparticles (bottom row)
Scale bars = 5 μm

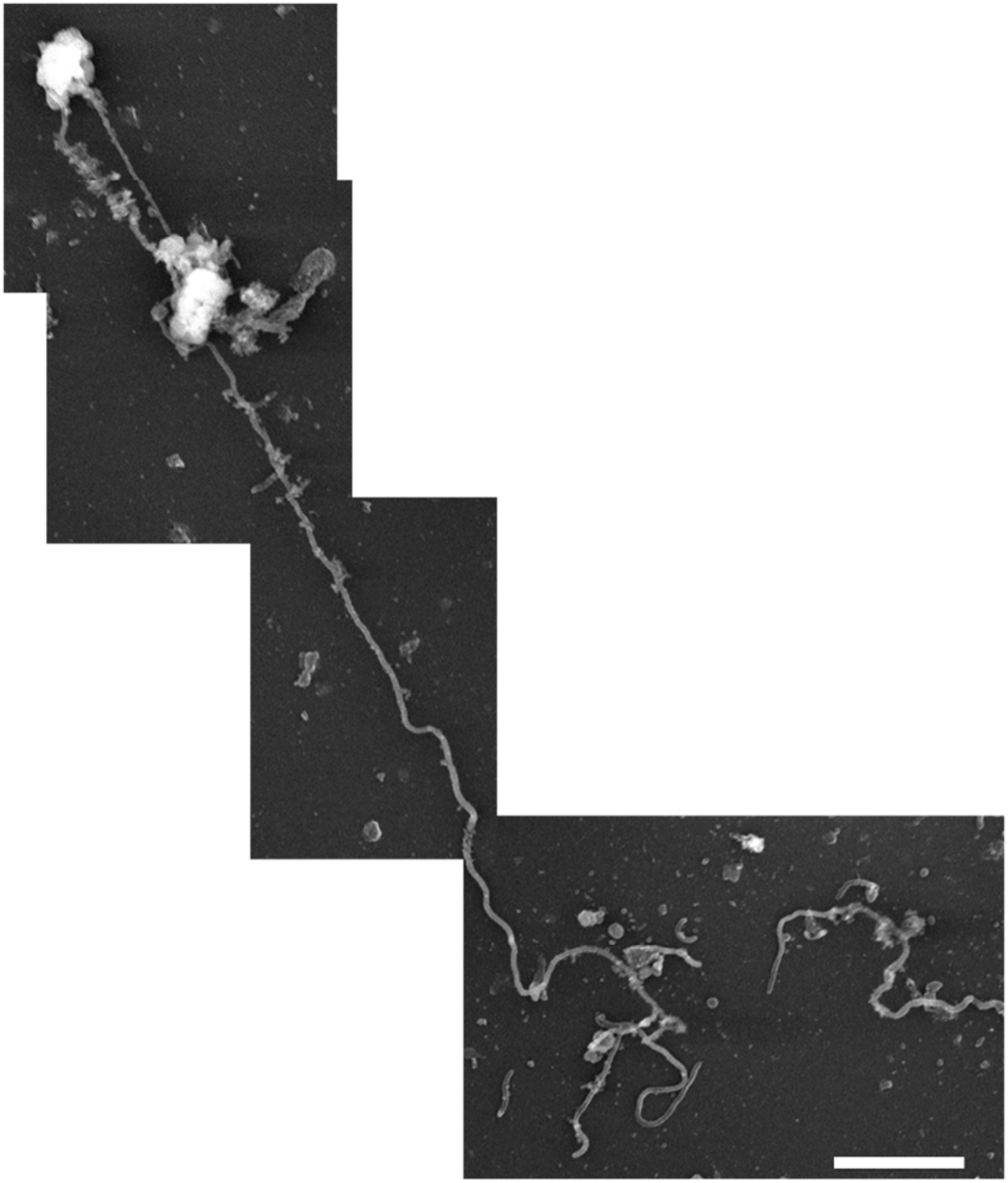

Figure A-3 continued. Combined Images of Elongated *Shewanella japonica* Cells after 14 d Incubation in Defined Culture Medium with Agarose
Coupon coated with polyurethane paint
Scale bar = 5 μm

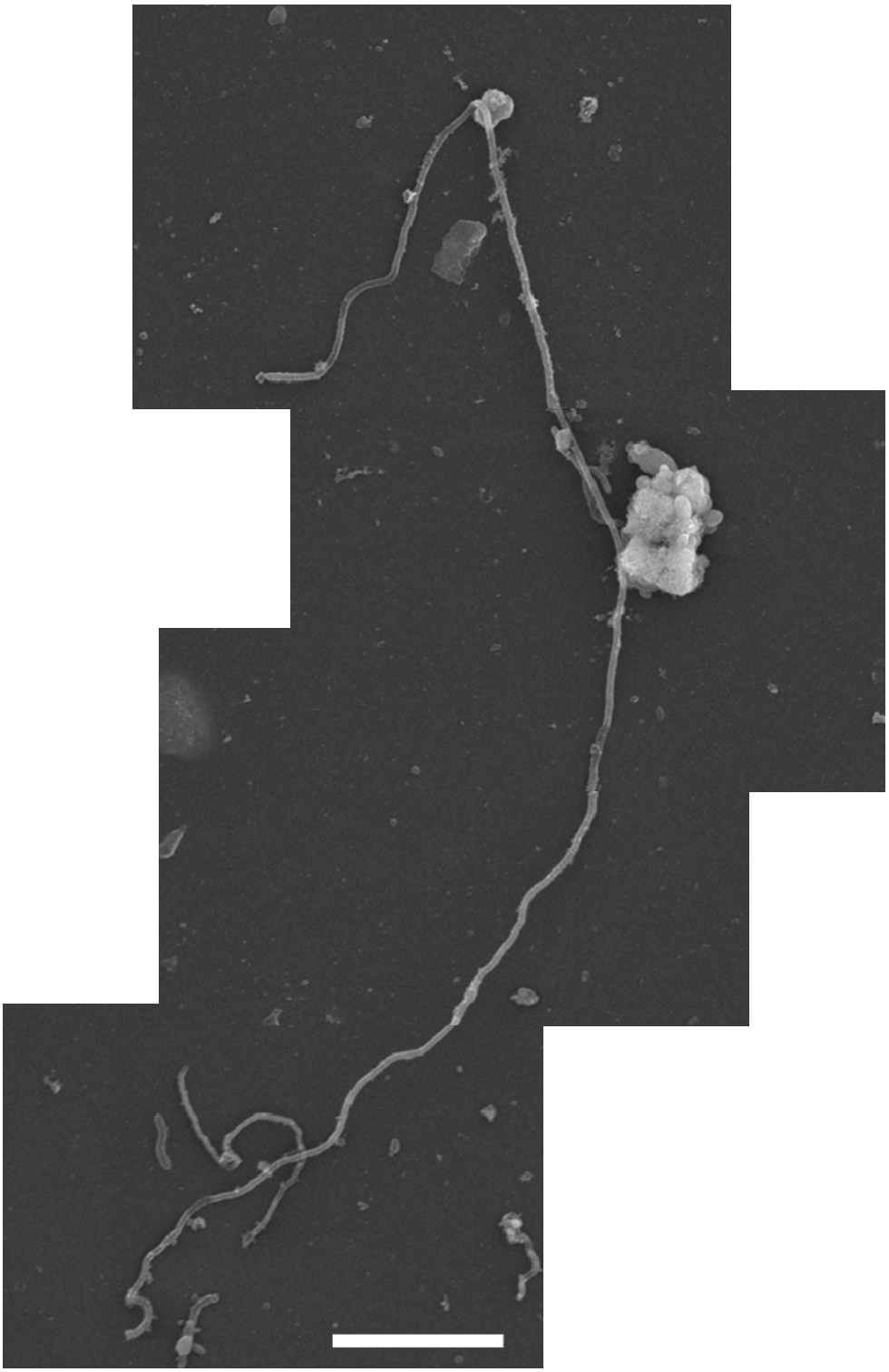

Figure A-3 continued. Combined Images of Elongated *Shewanella japonica* Cells after 14-d Incubation in Defined Culture Medium with Agarose
Coupon painted with polyurethane paint
Scale bar = 5 μm

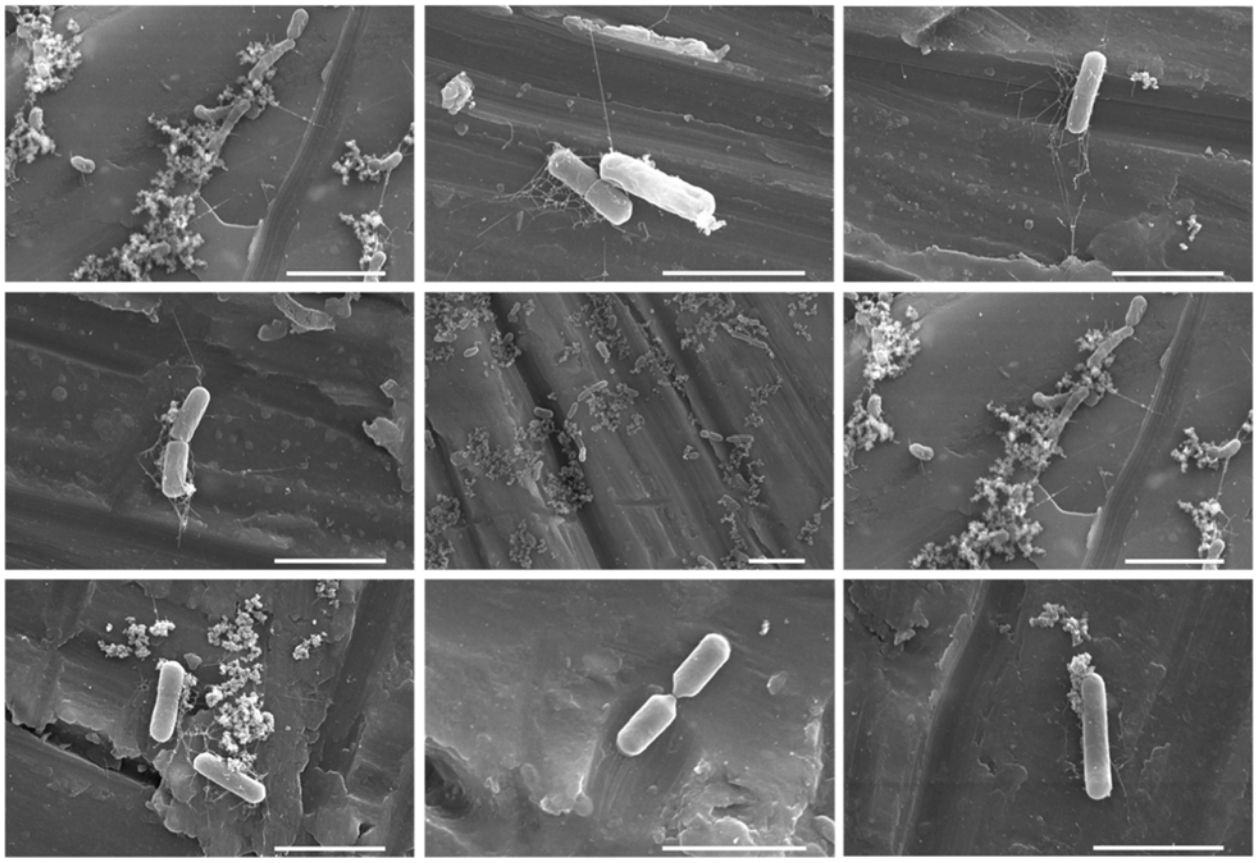

Figure 14. *Shewanella japonica* Cells after 1-d Incubation in Dilute Marine Broth 2216
All coupons unpainted
Scale bars = 5 µm

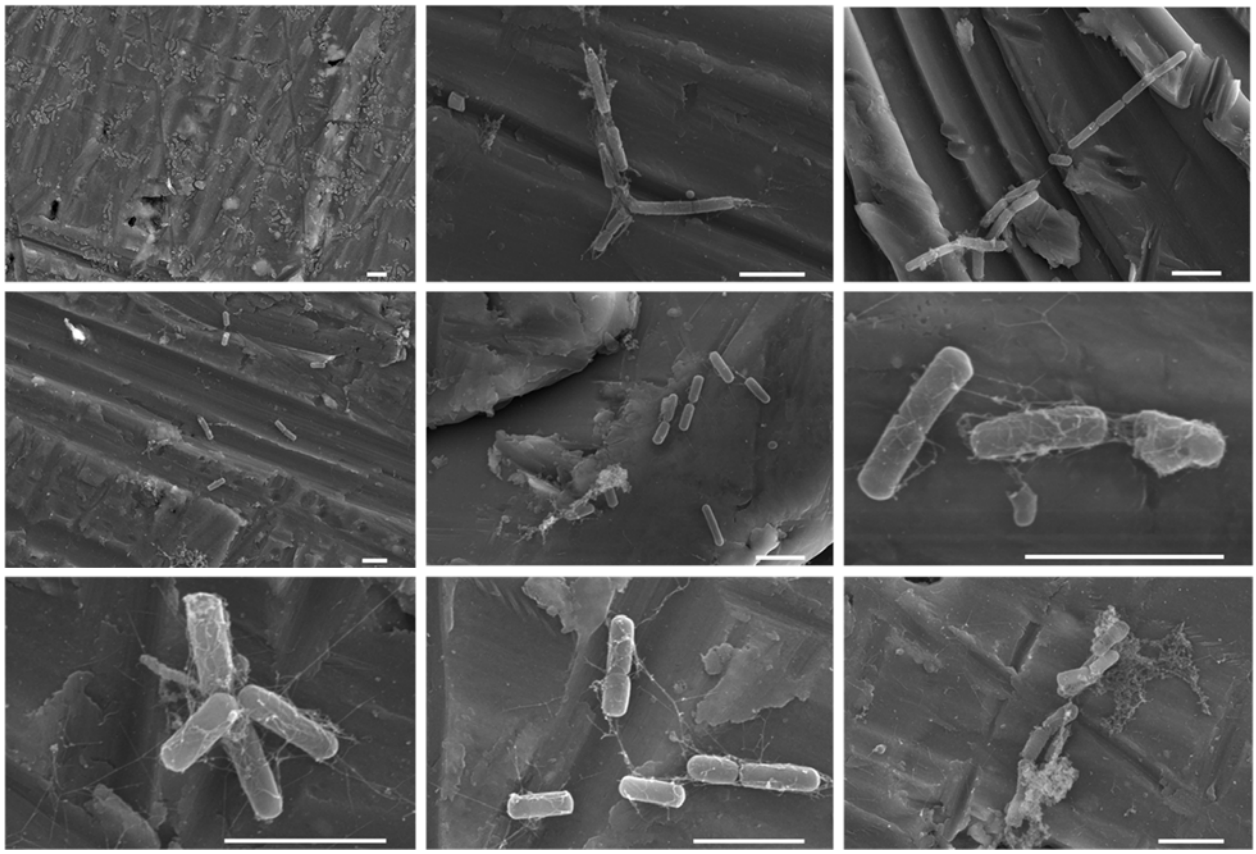

Figure 15. *Shewanella japonica* Cells after 2-d Incubation in Dilute Marine Broth 2216
All coupons unpainted
Scale bars = 5 μm

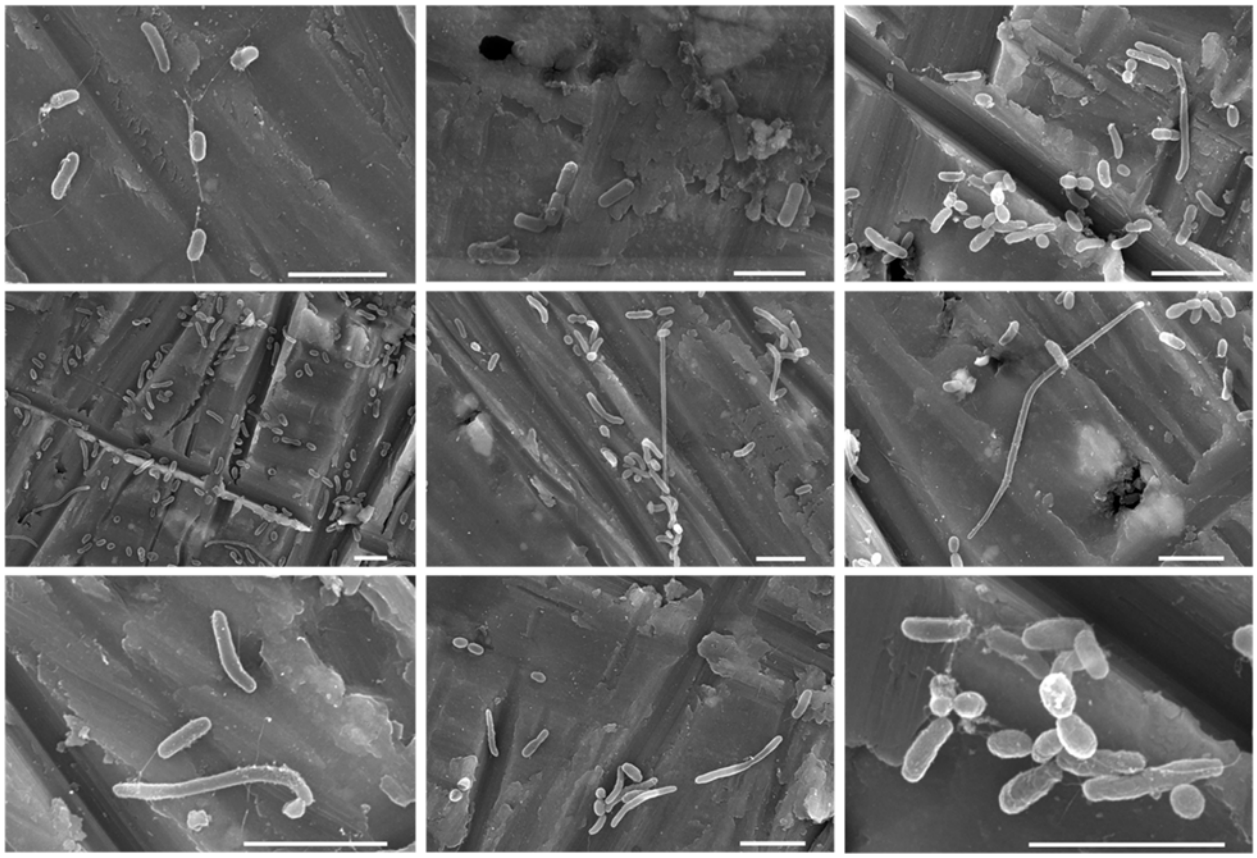

Figure 16. *Shewanella japonica* Cells after 3-d Incubation in Dilute Marine Broth 2216
All coupons unpainted
Scale bars = 5 µm

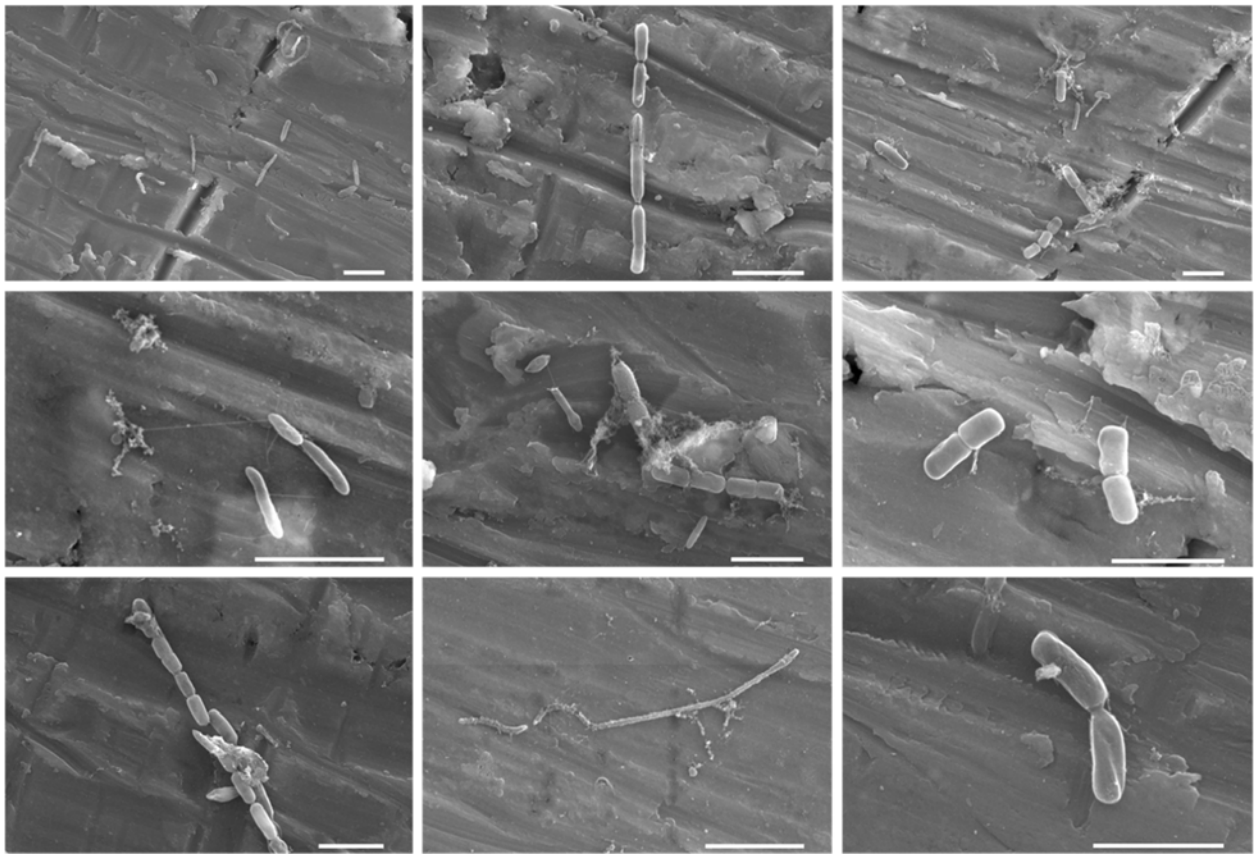

Figure 17. *Shewanella japonica* Cells after 6-d Incubation in Dilute Marine Broth 2216
All coupons unpainted
Scale bars = 5 µm

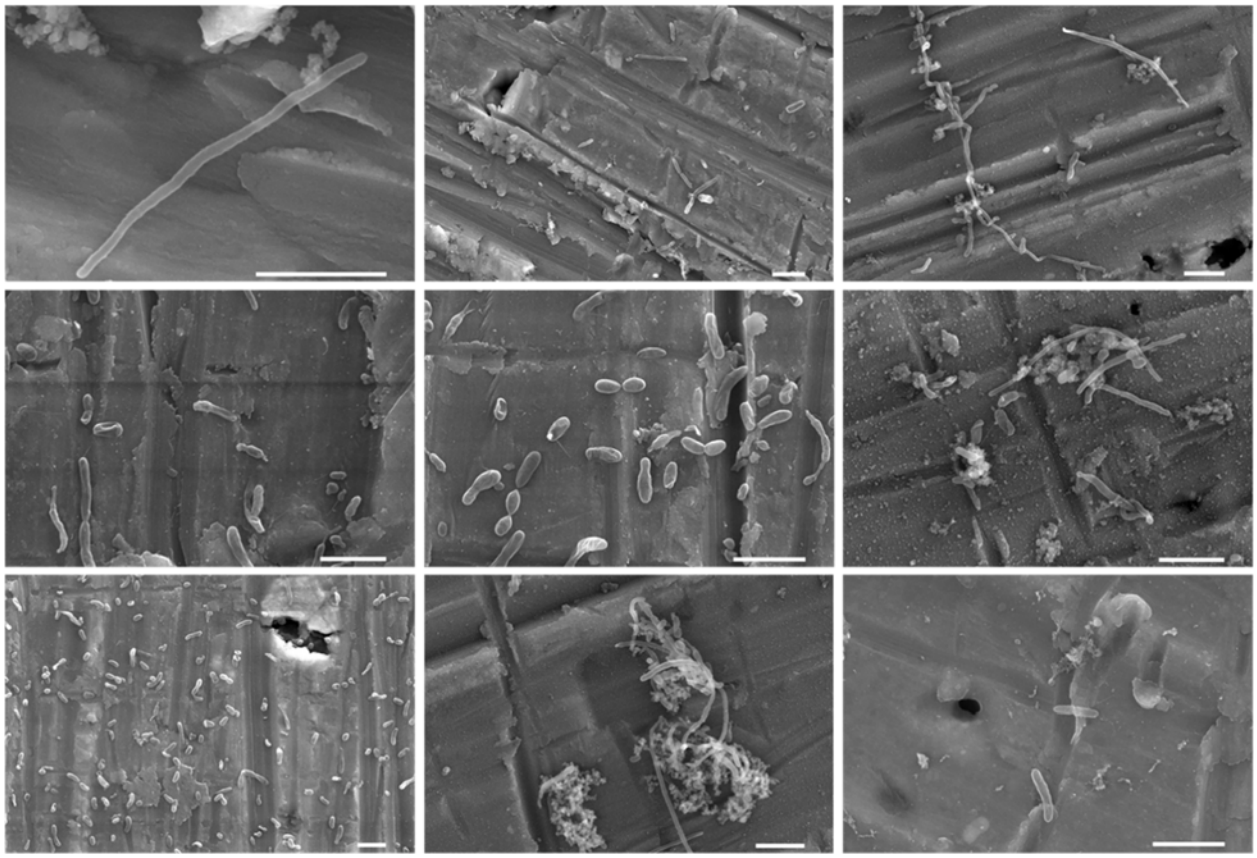

Figure 18. *Shewanella japonica* Cells after 7-d Incubation in Dilute Marine Broth 2216
All coupons unpainted
Scale bars = 5 µm

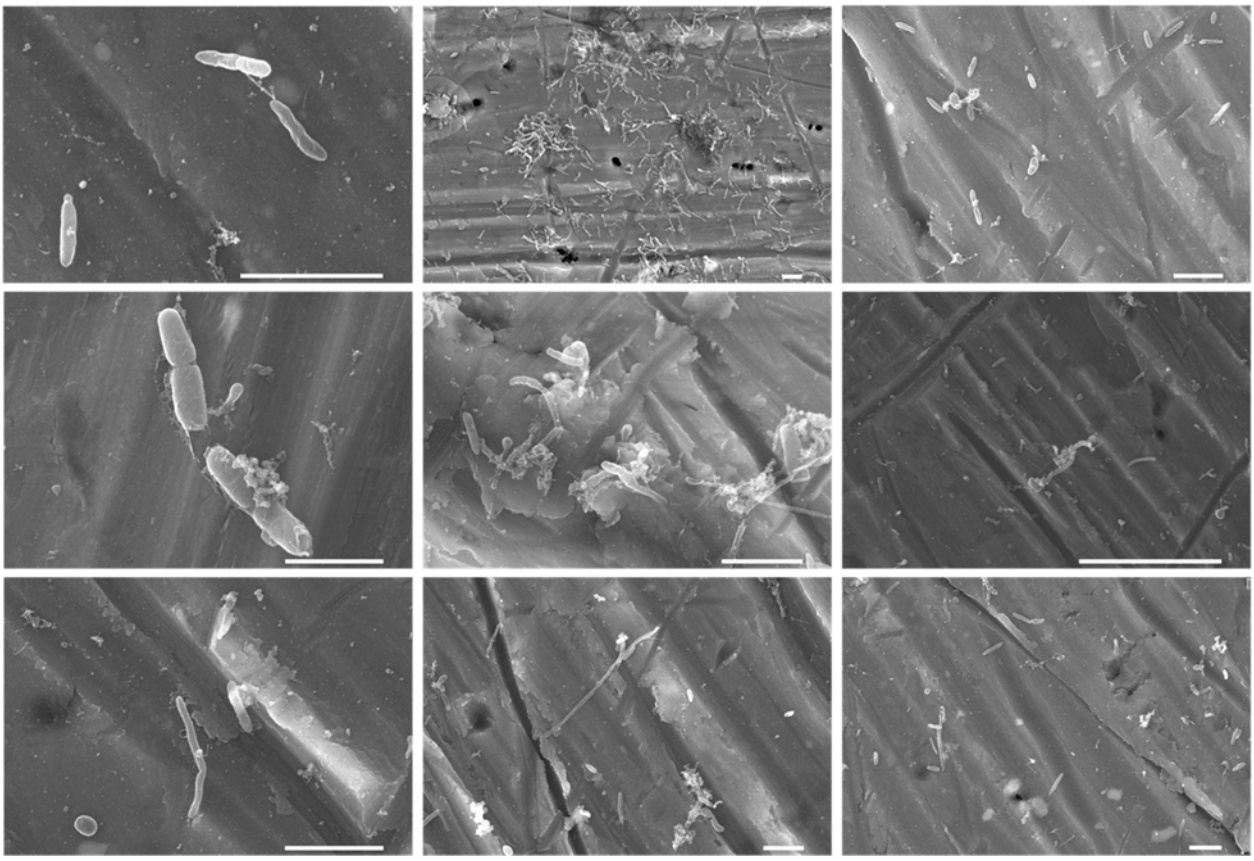

Figure 19. *Shewanella japonica* Cells after 14 d Incubation in Dilute Marine Broth 2216
All coupons unpainted
Scale bars = 5 µm